

# From transition electromagnetic form factors $\gamma^*\gamma^*\eta_c(1S, 2S)$ to the production of $\eta_c(1S, 2S)$ at the LHC\*

ANTONI SZCZUREK

Institute of Nuclear Physics Polish Academy of Sciences,  
ul. Radzikowskiego 152, PL-31342 Kraków, Poland,  
Faculty of Mathematics and Natural Sciences, University of Rzeszów,  
ul. Pigonia 1, PL-35-310 Rzeszów, Poland

We review our recent results for production of  $\eta_c(1S)$  and  $\eta_c(2S)$  in the  $\gamma^*\gamma^* \rightarrow \eta_c(1S, 2S)$  fusion and in proton-proton collisions via gluon-gluon fusion. The quarkonium wave functions are calculated by solving Schrödinger equation for different  $c\bar{c}$  potentials. Using Terentev prescription the light-cone wave functions are obtained. The light-cone wave functions are used then to calculate  $\gamma^*\gamma^* \rightarrow \eta_c$  transition form factors. The theoretical results are compared to the Belle experimental data for  $\eta_c(1S)$ . In addition we discuss our results for two-photon decay width. We present also results of our calculations for proton-proton collisions obtained within  $k_T$ -factorization approach for different unintegrated gluon distributions. The results for hadroproduction of  $\eta_c(1S)$  are compared to the LHCb experimental data.

PACS numbers: 12.38.-t, 12.39.Hg, 12.39.Ki, 12.39.Pn, 14.40.Pq

## 1. Introduction

There has been a lot of interest recently in the exclusive production of mesons via photon-photon fusion processes studied mainly at the  $e^+e^-$  colliders. Such studies were motivated by the expectation that at large photon virtualities the measurements of the cross sections provide strong constrains in the probability amplitude for finding partons in the mesons [1, 2, 3]. The meson - photon transition form factors are also of interest because of the role they play in the hadronic light-by-light contribution to the muon anomalous magnetic moment [4].

---

\* Presented at XXVI Cracow EIPhANY Conference, LHC Physics: Standard Model and Beyond, 7-10 January 2020

A lot of attention has been paid to the case of pseudoscalar light meson motivated by the experimental data from the CLEO, BaBar, Belle and L3 Collaborations for the  $\pi^0$ ,  $\eta$  and  $\eta'$  production in  $e^+e^-$  collisions. These collaborations extracted the transition form factor from single - tag events where only one of the leptons in the final state is measured. In this case, one of the photons is far off the mass shell, while the other is almost real. Such data allow to test the collinear factorization approach and the onset of the asymptotic regime, as well motivated the improvement of the theoretical approaches.

Similar results have been obtained for the  $\eta_c$  production. In this case, the  $\eta_c$  mass provides a hard scale that justifies to use a perturbative approach even for zero virtualities. In the past this transition form factor was studied in different approaches, (although often only for one virtual photon), such as: perturbative QCD [5, 6], lattice QCD [7, 8], non-relativistic QCD [9, 10], QCD sum rules [11], as well as from Dyson-Schwinger and Bethe-Salpeter equations [12]. In the light-front quark model (LFQM) the case of one virtual and one real photon has been studied in [13, 14].

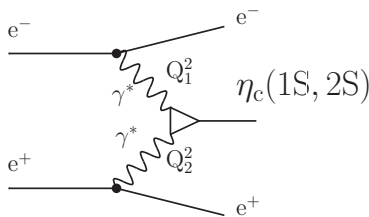


Fig. 1. Basic diagram for the  $\gamma^*\gamma^* \rightarrow \chi_c$  coupling.

The quarkonia production reactions in hadronic collisions is also very interesting (see e.g. [16]). In Ref.[17], we concentrated on the direct hadroproduction of the ground state of the charmonium family,  $\eta_c(1S)$ , and its first excited state  $\eta_c(2S)$ . Both are pseudoscalar particles of even charge parity  $J^{PC} = 0^{-+}$ . Like other  $C$ -even quarkonia, the dominant production mechanism is through the  $gg \rightarrow \mathcal{Q}$  gluon fusion  $2 \rightarrow 1$  process. For comparison in the standard collinear-factorization approach one must go to next-to-leading order (NLO) approximation to calculate the transverse momentum distribution of the quarkonium state and include  $2 \rightarrow 2$  processes like  $gg \rightarrow \mathcal{Q}g$ . In the  $k_T$ -factorization approach [18, 19, 20], the transverse momentum of the quarkonium originates from the transverse momenta of incident virtual gluons entering the hard  $g^*g^* \rightarrow \mathcal{Q}$  process.

The  $k_T$ -factorization approach is especially appropriate in the high-energy kinematics, where partons carry small momentum fractions of the incoming protons, mainly discussed in the framework of the BFKL formal-

ism [21]. In our recent calculations we adopted [17] the color-singlet model, which treats the quarkonium as a two-body bound state of a heavy quark and antiquark. Such a formalism was used previously for the production of  $\chi_{cJ}$  ( $J = 0, 1, 2$ ) quarkonia (see e.g. Ref. [22]), and a relatively good agreement with data was obtained from an unintegrated gluon distribution (UGD), which effectively includes the higher-order contributions.

## 2. $\gamma^*\gamma^* \rightarrow \eta_c$ coupling

### 2.1. Nonrelativistic quarkonium wave functions

The radial spatial wave functions were obtained by solving the Schrödinger equation [23]. Different potential models known from the literature were used. The momentum wave functions can be obtained then by calculating Fourier transform from the spatial wave functions. In Fig.2 we show the resulting wave functions. One can observe some dependence on the potential used in the calculation.

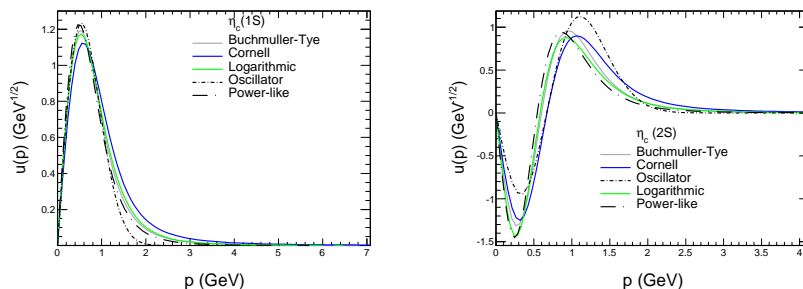


Fig. 2. Radial momentum-space wave function for different potentials.

In our approach we treat the  $\eta_c$  meson as a bound state of a charm quark and antiquark, assuming that the dominant contribution comes from the  $c\bar{c}$  component in the Fock-state expansion:

$$|\eta_c; P_+, \mathbf{P}\rangle = \sum_{i,j,\lambda,\bar{\lambda}} \frac{\delta_j^i}{\sqrt{N_c}} \int \frac{dz d^2\mathbf{k}}{z(1-z)16\pi^3} \Psi_{\lambda\bar{\lambda}}(z, \mathbf{k}) |c_{i\lambda}(zP_+, \mathbf{p}_c) \bar{c}_{\bar{\lambda}}^j((1-z)P_+, \mathbf{p}_{\bar{c}})\rangle + \dots \quad (1)$$

Here the  $c$ -quark and  $\bar{c}$ -antiquark carry a fraction  $z$  and  $1-z$  respectively of the  $\eta_c$ 's plus-momentum. The light-front helicities of quark and antiquark are denoted by  $\lambda, \bar{\lambda}$ , and take values  $\pm 1$ . The transverse momenta of quark and antiquark are

$$\mathbf{p}_c = \mathbf{k} + z\mathbf{P}, \quad \mathbf{p}_{\bar{c}} = -\mathbf{k} + (1-z)\mathbf{P}. \quad (2)$$

The light-cone representation is obtained by Terentev's prescription [25] valid for weakly bound systems.

The resulting light-cone wave functions are shown in Fig.3 for a selected  $c\bar{c}$  potential specified in the figure caption. According to the Terentev pre-

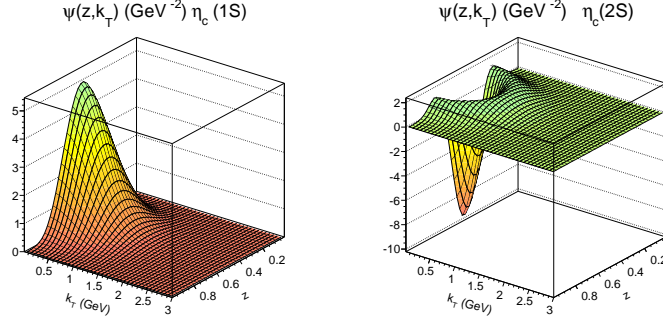


Fig. 3. Radial light-front wave function for Buchmüller-Tye potential.

scription [25]:  $\Rightarrow \mathbf{p} = \mathbf{k}, \quad p_z = (z - \frac{1}{2})M_{c\bar{c}},$

$$\psi(z, \mathbf{k}) = \frac{\pi}{\sqrt{2M_{c\bar{c}}}} \frac{u(p)}{p}.$$

The value of the transition form factor at  $Q_1^2, Q_2^2 = 0$  can be calculated as:

$$F(0, 0) = e_c^2 \sqrt{N_c} 4m_c \cdot \int \frac{dz d^2\mathbf{k}}{z(1-z)16\pi^3} \frac{\psi(z, \mathbf{k})}{\mathbf{k}^2 + m_c^2}.$$

$F(0, 0)$  is related to the two-photon decay width:

$$\Gamma(\eta_c \rightarrow \gamma\gamma) = \frac{\pi}{4} \alpha_{\text{em}}^2 M_{\eta_c}^3 |F(0, 0)|^2.$$

$F(0, 0)$  can be rewritten in the terms of radial momentum space wave function  $u(p)$ :

$$F(0, 0) = e_c^2 \sqrt{2N_c} \frac{2m_c}{\pi} \int_0^\infty \frac{dp p u(p)}{\sqrt{M_{c\bar{c}}^3(p^2 + m_c^2)}} \frac{1}{2\beta} \log\left(\frac{1+\beta}{1-\beta}\right),$$

In the non-relativistic (NR) limit, where  $p^2/m_c^2 \ll 1, \beta \ll 1$ , and  $2m_c = M_{c\bar{c}} = M_{\eta_c}$ , we obtain

$$F(0, 0) = e_c^2 \sqrt{N_c} \sqrt{2} \frac{4}{\pi \sqrt{M_{\eta_c}^5}} \int_0^\infty dp p u(p) = e_c^2 \sqrt{N_c} \frac{4 R(0)}{\sqrt{\pi M_{\eta_c}^5}},$$

where  $\beta = \frac{p}{\sqrt{p^2+m_c^2}}$ , the velocity  $v/c$  of the quark in the  $c\bar{c}$  cms-frame and  $R(0)$  radial wave function at the origin.

### 2.2. Results

In Table 1 below we show an example of our results for  $F(0,0)$ . In Ref.[15] we showed also results for  $\eta_c(2S)$ .

Table 1. Transition form factor  $|F(0,0)|$  for  $\eta_c(1S)$  at  $Q_1^2 = Q_2^2 = 0$ .

potential type	$m_c$ [GeV]	$ F(0,0) $ [GeV <sup>-1</sup> ]	$\Gamma_{\gamma\gamma}$ [keV]	$f_{\eta_c}$ [GeV]
harmonic oscillator	1.4	0.051	2.89	0.2757
logarithmic	1.5	0.052	2.95	0.3373
power-like	1.334	0.059	3.87	0.3074
Cornell	1.84	0.039	1.69	0.3726
Buchmüller-Tye	1.48	0.052	2.95	0.3276
experiment	-	$0.067 \pm 0.003$ [1]	$5.1 \pm 0.4$ [1]	$0.335 \pm 0.075$ [2]

Let us start presentation of our results for transition form factor for one real and one virtual photon. Such objects are measured for single-tagged  $e^+e^- \rightarrow e^+e^-\eta_c(1S)$  reaction, i.e. when only one scattered electron/positron is measured. In Fig.4 we show results of our calculations for different wave functions (potentials) for  $\eta_c(1S)$ . For comparison we show also experimental form factor extracted by the Babar collaboration [24]. The theoretical results depend on the potential used. For some models the agreement is better than for the other models. As discussed in [15], the results depend rather on the mass of the charm quark/antiquark and much less on particular form of the  $c\bar{c}$  potential.

In Fig.5 we show the dependence of the transition form factors on both photon virtualities for  $\eta_c(1S)$  (left panel) and  $\eta_c(2S)$  (right panel) as an example for the Buchmüller-Tye potential. Such distributions were shown in [15] for the first time.

In Fig.6 we show the form factors in slightly different representation:

$$\omega = \frac{Q_1^2 - Q_2^2}{Q_1^2 + Q_2^2} \text{ and } \bar{Q}^2 = \frac{Q_1^2 + Q_2^2}{2}.$$

We observe scaling in the  $\omega$  variable.

The convergence of  $Q^2F(Q^2)$  to its asymptotic value is shown in Fig.7 for different potentials used in [15]. Even at  $Q^2 \sim 30 \text{ GeV}^2$  our results is very far for the asymptotic value (different for different wave functions). The effect of RGE was discussed in [15] and was shown to be very slow.

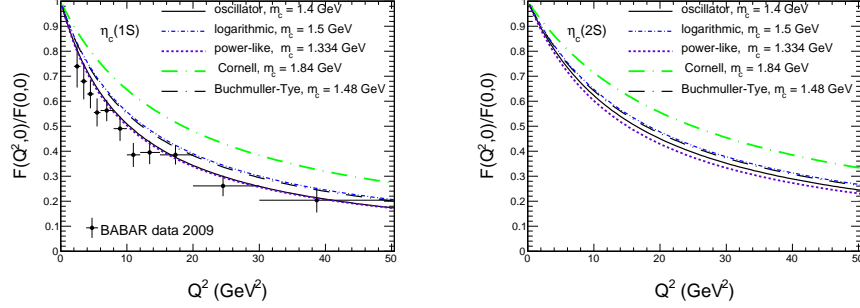


Fig. 4. Normalized transition form factor  $\tilde{F}(Q^2, 0)$  as a function of photon virtuality  $Q^2$ . The BaBar data are shown for comparison (see J. P. Lees *et al.* [24] [BaBar Collaboration]).

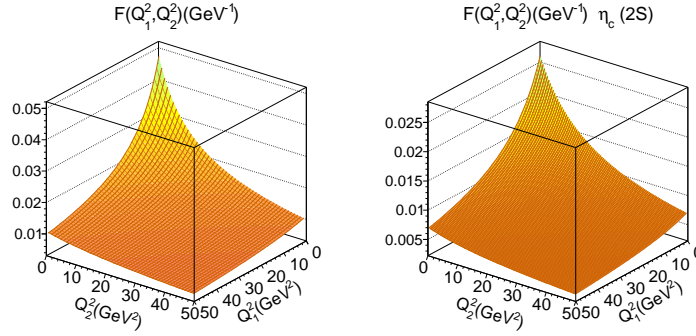


Fig. 5. Transition form factor for  $\eta_c(1S)$  and  $\eta_c(2S)$  for Buchmüller-Tye potential. The  $F(Q_1^2, Q_2^2)$  should obey Bose symmetry.

### 3. Inclusive production of $\eta_c$ quarkonia in proton-proton collisions

#### 3.1. Theoretical approach

The diagram shown in Fig.8 illustrates the situation adequate for the  $k_T$ -factorization calculations used in Ref.[17].

The inclusive cross section for  $\eta_c$ -production via the  $2 \rightarrow 1$  gluon-gluon fusion mode is obtained from

$$d\sigma = \int \frac{dx_1}{x_1} \int \frac{d^2\mathbf{q}_1}{\pi\mathbf{q}_1^2} \mathcal{F}(x_1, \mathbf{q}_1^2) \int \frac{dx_2}{x_2} \int \frac{d^2\mathbf{q}_2}{\pi\mathbf{q}_2^2} \mathcal{F}(x_2, \mathbf{q}_2^2) \frac{1}{2x_1x_2s} |\overline{\mathcal{M}}|^2 d\Phi(2 \rightarrow 1). (3)$$

The unintegrated gluon distributions are normalized such, that in the DGLAP-

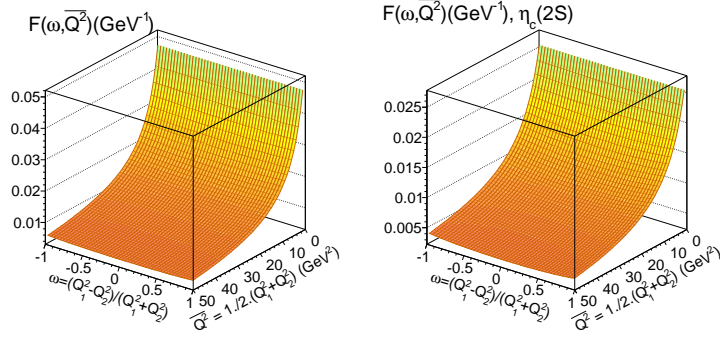


Fig. 6. The  $\gamma^*\gamma^* \rightarrow \eta_c(1S)$  and  $\gamma^*\gamma^* \rightarrow \eta_c(2S)$  form factor as a function of  $(\omega, Q^2)$  for the Buchmüller-Tye potential for illustration.

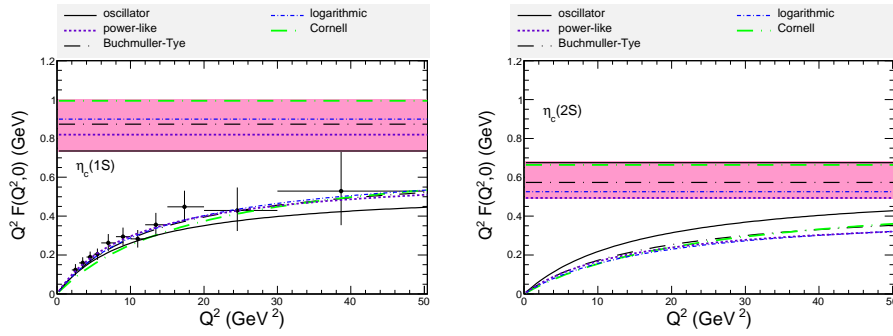


Fig. 7.  $Q^2 F(Q^2, 0)$  as a function of photon virtuality  $Q^2$ . The horizontal lines  $\frac{8}{3} f_{\eta_c}$  are shown for reference.

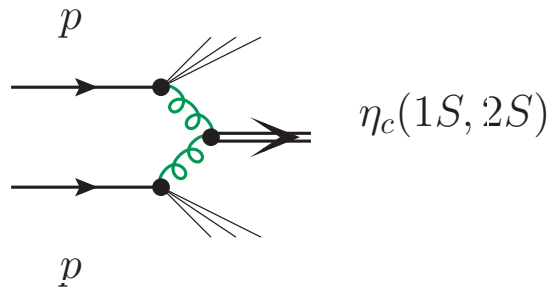


Fig. 8. Generic diagram for the inclusive process of  $\eta_c(1S)$  or  $\eta_c(2S)$  production in  $pp$  scattering via two gluons fusion.

limit

$$\mathcal{F}(x, \mathbf{q}^2) = \frac{\partial x g(x, \mathbf{q}^2)}{\partial \log \mathbf{q}^2}. \quad (4)$$

Let us denote the four-momentum of the  $\eta_c$  by  $P$ . It can be parametrized as:

$$P = (P_+, P_-, \mathbf{P}) = \left( \frac{m_\perp}{\sqrt{2}} e^y, \frac{m_\perp}{\sqrt{2}} e^{-y}, \mathbf{P} \right), \quad (5)$$

We therefore obtain for the inclusive cross section

$$\frac{d\sigma}{dy d^2 \mathbf{P}} = \int \frac{d^2 \mathbf{q}_1}{\pi \mathbf{q}_1^2} \mathcal{F}(x_1, \mathbf{q}_1^2) \int \frac{d^2 \mathbf{q}_2}{\pi \mathbf{q}_2^2} \mathcal{F}(x_2, \mathbf{q}_2^2) \delta^{(2)}(\mathbf{q}_1 + \mathbf{q}_2 - \mathbf{P}) \frac{\pi}{(x_1 x_2 s)^2} \overline{|\mathcal{M}|^2}, \quad (6)$$

where the momentum fractions  $x_{1,2}$  of gluons are

$$x_1 = \frac{m_\perp}{\sqrt{s}} e^y, \quad x_2 = \frac{m_\perp}{\sqrt{s}} e^{-y}. \quad (7)$$

The off-shell color singlet matrix element is written in terms of the Feynman amplitude as:

$$\mathcal{M}^{ab} = \frac{q_{1\perp}^\mu q_{2\perp}^\nu}{|\mathbf{q}_1||\mathbf{q}_2|} \mathcal{M}_{\mu\nu}^{ab} = \frac{q_{1+} q_{2-}}{|\mathbf{q}_1||\mathbf{q}_2|} n_\mu^+ n_\nu^- \mathcal{M}_{\mu\nu}^{ab} = \frac{x_1 x_2 s}{2|\mathbf{q}_1||\mathbf{q}_2|} n_\mu^+ n_\nu^- \mathcal{M}_{\mu\nu}^{ab}. \quad (8)$$

Then, we obtain for the cross section

$$\frac{d\sigma}{dy d^2 \mathbf{P}} = \int \frac{d^2 \mathbf{q}_1}{\pi \mathbf{q}_1^4} \mathcal{F}(x_1, \mathbf{q}_1^2) \int \frac{d^2 \mathbf{q}_2}{\pi \mathbf{q}_2^4} \mathcal{F}(x_2, \mathbf{q}_2^2) \delta^{(2)}(\mathbf{q}_1 + \mathbf{q}_2 - \mathbf{P}) \frac{\pi}{4} \overline{|n_\mu^+ n_\nu^- \mathcal{M}_{\mu\nu}^{ab}|^2}, \quad (9)$$

It is related to the  $\gamma^* \gamma^* \eta_c$  transition form factor through the relation

$$F(Q_1^2, Q_2^2) = e_c^2 \sqrt{N_c} I(\mathbf{q}_1^2, \mathbf{q}_2^2). \quad (10)$$

The vector product  $[\mathbf{q}_1, \mathbf{q}_2]$  is defined as

$$[\mathbf{q}_1, \mathbf{q}_2] = q_1^x q_2^y - q_1^y q_2^x = |\mathbf{q}_1||\mathbf{q}_2| \sin(\phi_1 - \phi_2). \quad (11)$$

Then, the averaged matrix element squared becomes

$$\begin{aligned} \overline{|n_\mu^+ n_\nu^- \mathcal{M}_{\mu\nu}^{ab}|^2} &= 16\pi^2 \alpha_S^2 \frac{1}{4} \frac{1}{N_c} |[\mathbf{q}_1, \mathbf{q}_2] I(\mathbf{q}_1^2, \mathbf{q}_2^2)|^2 \frac{1}{(N_c^2 - 1)^2} \sum_{a,b} \delta^{ab} \delta^{ab} \\ &= 4\pi^2 \alpha_S^2 \frac{1}{N_c(N_c^2 - 1)} |[\mathbf{q}_1, \mathbf{q}_2] I(\mathbf{q}_1^2, \mathbf{q}_2^2)|^2 \end{aligned} \quad (12)$$



Table 2. Total decay widths as well as  $|F(0,0)|$  obtained from  $\Gamma_{tot}$  using the next-to-leading order approximation.

	Experimental values	Derived from Eq.(16)
	$\Gamma_{tot}$ (MeV)	$ F(0,0) _{gg}[GeV^{-1}]$
$\eta_c(1S)$	$31.9 \pm 0.7$	$0.119 \pm 0.001$
$\eta_c(2S)$	$11.3 \pm 3.2 \pm 2.9$	$0.053 \pm 0.010$

This leads to our final result:

$$\frac{d\sigma}{dyd^2\mathbf{P}} = \int \frac{d^2\mathbf{q}_1}{\pi\mathbf{q}_1^4} \mathcal{F}(x_1, \mathbf{q}_1^2) \int \frac{d^2\mathbf{q}_2}{\pi\mathbf{q}_2^4} \mathcal{F}(x_2, \mathbf{q}_2^2) \delta^{(2)}(\mathbf{q}_1 + \mathbf{q}_2 - \mathbf{P}) \frac{\pi^3 \alpha_S^2}{N_c(N_c^2 - 1)} |[\mathbf{q}_1, \mathbf{q}_2] I(\mathbf{q}_1^2, \mathbf{q}_2^2)|^2.$$

In real calculation we take  $\mu_F^2 = m_T^2$  and for renormalization scale(s)

$$\alpha_s^2 \rightarrow \alpha_s(\max(m_t^2, q_{t,1}^2)) \alpha_s(\max(m_t^2, q_{t,2}^2)). \quad (13)$$

From the proportionality of the  $g^*g^*\eta_c$  and  $\gamma^*\gamma^*\eta_c$  vertices to the leading order (LO), we obtain, that at LO:

$$\Gamma_{LO}(\eta_c \rightarrow gg) = \frac{N_c^2 - 1}{4N_c^2} \frac{1}{e_c^4} \left( \frac{\alpha_s}{\alpha_{em}} \right)^2 \Gamma_{LO}(\eta_c \rightarrow \gamma\gamma), \quad (14)$$

where the LO  $\gamma\gamma$  width is related to the transition form factor for vanishing virtualities through

$$\Gamma_{LO}(\eta_c \rightarrow \gamma\gamma) = \frac{\pi}{4} \alpha_{em}^2 M_{\eta_c}^3 |F(0,0)|^2. \quad (15)$$

At NLO, the expressions for the widths read (see [26])

$$\begin{aligned} \Gamma(\eta_c \rightarrow \gamma\gamma) &= \Gamma_{LO}(\eta_c \rightarrow \gamma\gamma) \left( 1 - \frac{20 - \pi^2}{3} \frac{\alpha_s}{\pi} \right), \\ \Gamma(\eta_c \rightarrow gg) &= \Gamma_{LO}(\eta_c \rightarrow gg) \left( 1 + 4.8 \frac{\alpha_s}{\pi} \right). \end{aligned} \quad (16)$$

We use a few different UGDs which are available from the literature, e.g. from the TMDLib package (see [27]) or the CASCADE Monte Carlo code (see [28]).

1. Firstly we use a glue constructed according to the prescription initiated in Kimber et al.[29] and later updated in Martin et al.[30]), which we label below as ‘‘KMR’’. It uses as an input the collinear gluon distribution from Harland-Lang et al.[31].

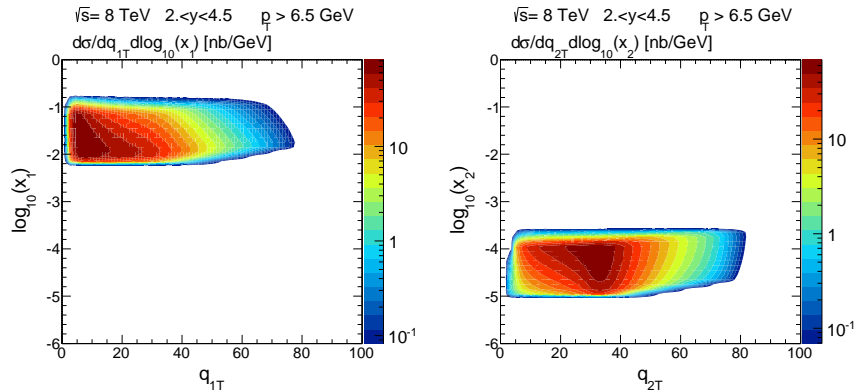


Fig. 9. Two-dimensional distributions in  $(x_1, q_{1T})$  (left panel) and in  $(x_2, q_{2T})$  (right panel) for  $\eta_c(1S)$  production for  $\sqrt{s} = 8$  TeV. In this calculation the KMR UGD was used for illustration.

2. Secondly, we employ two UGDs obtained by Kutak [32]. There are two versions of this UGD. Both introduce a hard scale dependence via a Sudakov form factor into solutions of a small- $x$  evolution equation. The first version uses the solution of a linear, BFKL evolution with a resummation of subleading terms and is denoted by "Kutak (linear)". The second UGD, denoted as "Kutak (nonlinear)" uses instead a nonlinear evolution equation of Balitsky-Kovchegov type. Both of the Kutak's UGDs [32] can be applied only in the small- $x$  regime,  $x < 0.01$ .
3. The third type of UGD has been obtained by Hautmann and Jung from a description of precise HERA data on deep inelastic structure function by a solution of the CCFM evolution equations. We use "Set 2". from [33].

### 3.2. Results

In Fig.9 we show the cross section distributions for  $(x_1, q_{1T})$  (left panel) and  $(x_2, q_{2T})$  (right panel). For the LHCb kinematics the two distributions are not identical:  $x_1 \gg x_2$  and on average  $q_{1T} < q_{2T}$ .

The projections on longitudinal momentum fraction and gluon transverse momentum squared are shown in the left and right panels of Fig.10.

Transverse momentum distributions for  $\eta_c(1S)$  are shown in Fig.11 for three different collision energies for different unintegrated gluon distributions specified in the figure. The LHCb data points are shown for comparison. Our theoretical results almost agree with the LHCb data for  $\sqrt{s} =$

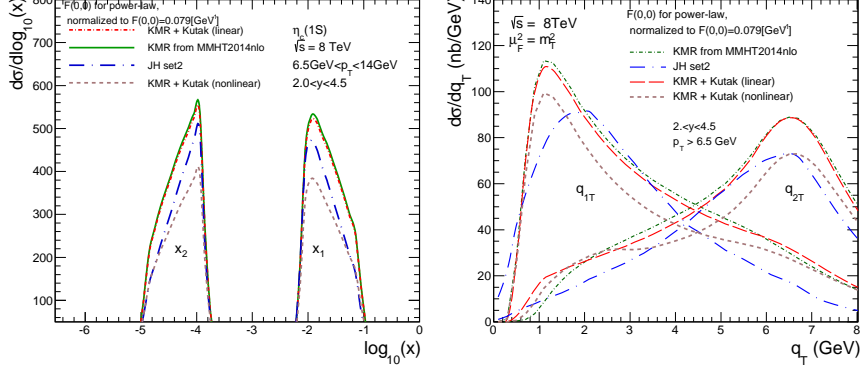


Fig. 10. Distributions in  $\log_{10}(x_1)$  or  $\log_{10}(x_2)$  (left panel) and distributions in  $q_{1T}$  or  $q_{2T}$  (right panel) for the LHCb kinematics. Here the selected UGDs were used in our calculations. Here we show an example for  $\sqrt{s} = 8$  TeV.

7 and 8 TeV while at  $\sqrt{s} = 13$  TeV the preliminary experimental data are above our predictions. We have no idea how to explain the disagreement.

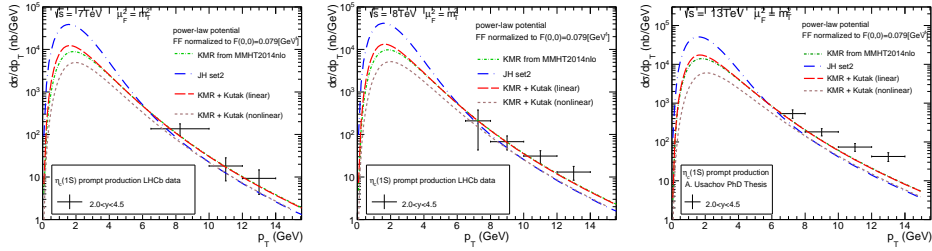


Fig. 11. Differential cross section as a function of transverse momentum for prompt  $\eta_c(1S)$  production compared with the LHCb data (see [34]) for  $\sqrt{s} = 7, 8$  TeV and preliminary experimental data (Usachov PhD [35]) for  $\sqrt{s} = 13$  TeV. Different UGDs were used. Here we used the  $g^*g^* \rightarrow \eta_c(1S)$  form factor calculated from the power-law potential.

Our predictions for  $\eta_c(2S)$  are shown in Fig.12. The shapes of the distributions are similar to those for  $\eta_c(1S)$  while the cross section is slightly smaller.

The dependence on form factors are shown in Fig.13. In general our results are less uncertain as far as the form factor is considered compared to uncertainties due to unintegrated gluon distributions shown above.

Finally in Fig.14 we demonstrate how important is inclusion of form factor. The effect is huge. This puts into question all calculations in which the form factor is not included.

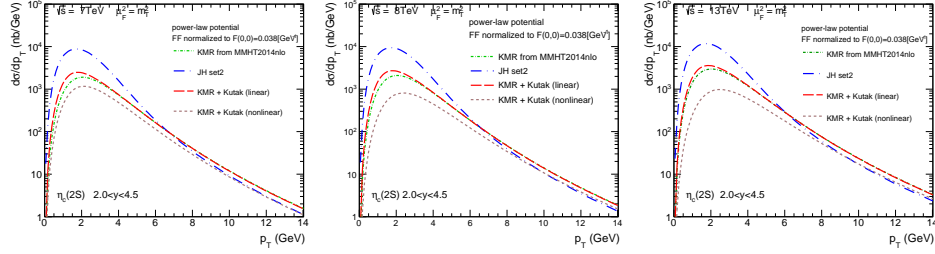


Fig. 12. Differential cross section as a function of transverse momentum for prompt production of  $\eta_c(2S)$  for  $\sqrt{s} = 7, 8, 13$  TeV.

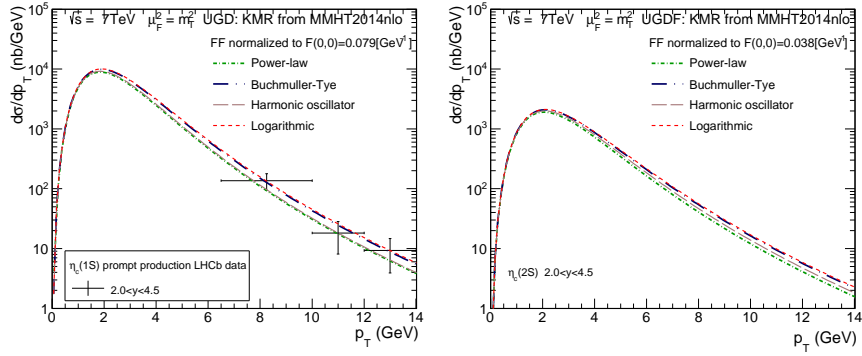


Fig. 13. Transverse momentum distributions calculated with different form factors obtained from different potential models of quarkonium wave function and one common normalization of  $|F(0, 0)|$ .

#### 4. Conclusion

Here we briefly summarize our results found in [15] and [17].

- The transition form factor for different wave functions obtained as a solution of the Schrödinger equation for the  $c\bar{c}$  system, for different phenomenological  $c\bar{c}$  potentials from the literature, was calculated.
- We studied the transition form factors for  $\gamma^*\gamma^* \rightarrow \eta_c(1S,2S)$  for two space-like virtual photons, which can be accessed experimentally in future measurements of the cross section for the  $e^+e^- \rightarrow e^+e^-\eta_c$  process in the double-tag mode.
- The transition form factor for only one off-shell photon as a function of its virtuality was studied and compared to the BaBar data for the  $\eta_c(1S)$  case.

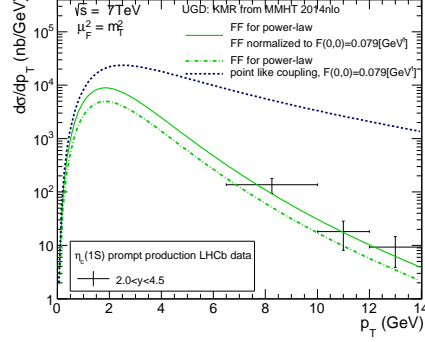


Fig. 14. Comparison of results for two different transition form factor, computed with the KMR unintegrated gluon distribution. We also show result when the  $(q_{1T}^2, q_{2T}^2)$  dependence of the transition form factor is neglected (short dashed line).

- Predictions for  $\eta_c(2S)$  were presented.
- Dependence of the transition form factor on the virtuality was studied and delayed convergence of the form factor to its asymptotic value  $\frac{8}{3}f\eta_c$  as predicted by the standard hard scattering formalism, was presented.
- There is practically no dependence of transition form factor on the asymmetry parameter  $\omega$ , which could be verified experimentally at Belle 2.
- The  $k_T$ -factorization approach with modern UGDs lead to good description of the LHCb data for  $pp \rightarrow \eta_c(1S) \rightarrow p\bar{p}$  for  $\sqrt{s} = 7, 8$  TeV and somewhat worse for  $\sqrt{s} = 13$  TeV. There is some room for color octet. Feed down contribution is small [36].
- Range of  $x_1, x_2$  and  $q_{1T}, q_{2T}$  was discussed. For the LHCb kinematics very small longitudinal momentum fractions are probed. Transverse momenta are not too small.
- We do not see an obvious sign of the onset of saturation. LHCb cross section grows even faster than our result without saturation. However the gluon transverse momenta are not small.
- Predictions for hadroproduction of  $\eta_c(2S)$  were also presented.
- We also discussed uncertainties related to  $g^*g^* \rightarrow \eta_c$  form factor. They are somewhat smaller than those related to UGDs.

Recently we have performed similar studies also for scalar quarkonium  $\chi_c(0)$  [37] and light  $f_0(980)$  meson [38].

### Acknowledgements

I would like to thank Iza Babiarz, Victor Goncalves, Roman Pasechnik and Wolfgang Schafer for collaboration on the topics presented in this short review. This study was partially supported by the Polish National Science Center grant UMO-2018/31/B/ST2/03537 and by the Center for Innovation and Transfer of Natural Sciences and Engineering Knowledge in Rzeszów.

### REFERENCES

- [1] A. V. Radyushkin, JINR-P2-10717 (Dubna, 1977), [hep-ph/0410276]; A. V. Efremov and A. V. Radyushkin, Theor. Math. Phys. **42**, 97 (1980) [Teor. Mat. Fiz. **42**, 147 (1980)]; Phys. Lett. **94B**, 245 (1980).
- [2] G. P. Lepage and S. J. Brodsky, Phys. Lett. **87B**, 359 (1979).
- [3] V. L. Chernyak and A. R. Zhitnitsky, Phys. Rept. **112**, 173 (1984).
- [4] F. Jegerlehner, Springer Tracts Mod. Phys. **274**, pp.1 (2017).
- [5] T. Feldmann and P. Kroll, Phys. Lett. B **413**, 410 (1997) [hep-ph/9709203].
- [6] F. G. Cao and T. Huang, Phys. Rev. D **59**, 093004 (1999) [hep-ph/9711284].
- [7] J.J. Dudek and R.G. Edwards, Phys. Rev. Lett. **97**, 172001 (2006).
- [8] T. Chen et al. (CLQCD collaboration), Eur. Phys. J. C **76**, 358 (2016).
- [9] F. Feng, Y. Jia and W.-L. Sang, Phys. Rev. Lett. **115**, 222001 (2015).
- [10] S.Q. Wang, X.G. Wu, W.-L. Sang and S.J. Brodsky, Phys. Rev. **D97**, 0094034 (2018).
- [11] W. Lucha and D. Melikhov, Phys. Rev. **D86**, 016001 (2012).
- [12] J. Chen, M. Ding, L. Chang and Y.-X. Liu, Phys. Rev. D **95**, 016010 (2017).
- [13] C.Q. Geng and C.C. Lih, Eur. Phys. J **73**, 25005 (2013).
- [14] H. Y. Ryu, H. M. Choi and C. R. Ji, Phys. Rev. D **98**, no.3, 034018 (2018) [arXiv:1804.08287 [hep-ph]].
- [15] I. Babiarz, V.P. Goncalves, R. Pasechnik, W. Schäfer and A. Szczurek, Phys.Rev. **D100** 054018 (2019)
- [16] J. P. Lansberg, “New Observables in Inclusive Production of Quarkonia,” arXiv:1903.09185 [hep-ph].
- [17] I. Babiarz, R. Pasechnik, W. Schäfer and A. Szczurek, JHEP **2002** (2020) 037.
- [18] L. V. Gribov, E. M. Levin and M. G. Ryskin, Phys. Rept. **100**, 1 (1983). E. M. Levin, M. G. Ryskin, Y. M. Shabelski and A. G. Shuvaev, Sov. J. Nucl. Phys. **53**, 657 (1991) [Yad. Fiz. **53**, 1059 (1991)].

- [19] S. Catani, M. Ciafaloni and F. Hautmann, Phys. Lett. B **242**, 97 (1990); Nucl. Phys. B **366**, 135 (1991); Phys. Lett. B **307**, 147 (1993).
- [20] J. C. Collins and R. K. Ellis, Nucl. Phys. B **360**, 3 (1991).
- [21] V. S. Fadin, E. A. Kuraev and L. N. Lipatov, Phys. Lett. **60B**, 50 (1975); I. I. Balitsky and L. N. Lipatov, Sov. J. Nucl. Phys. **28**, 822 (1978) [Yad. Fiz. **28**, 1597 (1978)]; L. N. Lipatov, Phys. Rept. **286**, 131 (1997) [hep-ph/9610276].
- [22] A. Cisek and A. Szczurek, Phys. Rev. D **97**, no. 3, 034035 (2018).
- [23] J. Cepila, J. Nemchik, M. Krelina and R. Pasechnik, arXiv:1901.02664 [hep-ph].
- [24] J. P. Lees *et al.* [BaBar Collaboration], Phys. Rev. D **81**, 052010 (2010) [arXiv:1002.3000 [hep-ex]].
- [25] M. V. Terentev, Sov. J. Nucl. Phys. **24**, 106 (1976) [Yad. Fiz. **24**, 207 (1976)].
- [26] J. P. Lansberg and T. N. Pham, Phys. Rev. D **74**, 034001 (2006); Phys. Rev. D **79**, 094016 (2009) [arXiv:0903.1562 [hep-ph]].
- [27] F. Hautmann, H. Jung, M. Krämer, P. J. Mulders, E. R. Nocera, T. C. Rogers and A. Signori, Eur. Phys. J. C **74**, 3220 (2014) [arXiv:1408.3015 [hep-ph]].
- [28] H. Jung *et al.*, Eur. Phys. J. C **70**, 1237 (2010) [arXiv:1008.0152 [hep-ph]].
- [29] M. A. Kimber, A. D. Martin and M. G. Ryskin, Phys. Rev. D **63**, 114027 (2001) [hep-ph/0101348].
- [30] A. D. Martin, M. G. Ryskin and G. Watt, Eur. Phys. J. C **66**, 163 (2010) [arXiv:0909.5529 [hep-ph]].
- [31] L. A. Harland-Lang, A. D. Martin, P. Motylinski and R. S. Thorne, Eur. Phys. J. C **75**, no. 5, 204 (2015) [arXiv:1412.3989 [hep-ph]].
- [32] K. Kutak, Phys. Rev. D **91**, no. 3, 034021 (2015).
- [33] F. Hautmann and H. Jung, Nucl. Phys. B **883**, 1 (2014) [arXiv:1312.7875 [hep-ph]].
- [34] R. Aaij *et al.* [LHCb Collaboration], Eur. Phys. J. C **75**, no. 7, 311 (2015).
- [35] A. Usachov, “Study of charmonium production using decays to hadronic final states with the LHCb experiment,” arXiv:1910.08796 [hep-ex].
- [36] S. P. Baranov and A. V. Lipatov, Eur. Phys. J. C **79**, no. 7, 621 (2019).
- [37] I. Babiarz, R. Pasechnik, W. Schäfer and A. Szczurek, arXiv:2002.09352.
- [38] P. Lebiedowicz, R. Maciula and A. Szczurek, arXiv:2003.08200.